

Statistical Maxwell's Electromagnetic Theories Applied to Imaging of Objects in Geophysical and Biological Media

Akira Ishimaru^{*}, Ce Zhang, and Yasuo Kuga

(Invited Paper)

Abstract—Statistical Maxwell's Electromagnetic Theories have been developed over many years and applied to a wide range of practical problems in remote sensing of geographical media, imaging in biological media, medical optics, ultrasound imaging, and object detection and imaging and communications in clutter environment. This paper gives a review of recent advances, development and applications of statistical wave theory. Many important problems on imaging in geophysical and biological media have been treated often as separate problems. This paper attempts to present unified theoretical work and viewpoints under the statistical theories which may help further advance and understanding of theories and applications. The statistical electromagnetic theories encompass most advanced mathematical and theoretical work and most practical applications. This includes time-reversal imaging through multiple scattering media, super resolution, communication channel capacity in clutter, space-time vector radiative transfer, bio-electromagnetics and ultrasound in tissues, coherence in multiple scattering, memory effects, the use of transformation electromagnetics, seismic coda, and the fundamental multiple scattering theories. Statistical Electromagnetics Theories are one of the most challenging theoretical problems today involving many applications in geographical and biological media.

1. INTRODUCTION

Maxwell's equations are the cornerstone of our profession. One of the important areas of the work of our profession is the statistical electromagnetic theories, which have a wide range of practical applications such as microwave remote sensing of the earth, object detection in clutter, medical optics and ultrasound imaging, characterization of metamaterials and composite materials, and wireless communications through clutter environments. There are numerous important practical problems in imaging and geophysical and biological media which have been studied often as separate problems. However, many of these problems belong to the statistical electromagnetic theories and the unified theoretical work and viewpoints under the statistical theories help to advance the work related to this field. Such unified treatments of seemingly disjoint problems are important and essential, and this paper attempts to present such approach on many theoretical and practical problems to help further advance and understanding of the statistical electromagnetic theories and applications. It should also be noted that the statistical electromagnetic theories encompass most advanced theoretical and mathematical work and most practical applications.

There have been great progress made in understanding statistical multiple scattering theories in random media and rough surfaces, which have been benefitted greatly from many studies made in quantum electrodynamics and astrophysics such as Feynman Diagrams, Wigner Distributions, Anderson Localizations and Dyson and Bethe-Salpeter equations [1–8].

Received 31 December 2014, Accepted 29 March 2015, Scheduled 31 March 2015

Invited paper for the Commemorative Collection on the 150-Year Anniversary of Maxwell's Equations.

^{*} Corresponding author: Akira Ishimaru (ishimaru@u.washington.edu).

The authors are with the Department of Electrical Engineering, University of Washington, Seattle, USA.

This paper gives a review of statistical electromagnetics theories and applications to imaging, probing and detection in random media. In many problems dealing with random media, it is important to have a clear understanding of the interaction of waves and media. Many natural geographical and biological media are randomly varying in space and time and the wave propagating through such media experience random variation of amplitude and phase. Examples are the atmosphere, the ocean, terrain, planetary atmosphere, and interstellar turbulence. Biological media, tissue and blood, affect the wave scattering and imaging. The study of statistical electromagnetic theories are important for many environmental and health concerns including climate, hydrological, water, agricultural and ocean, thermal emissions, soil moistures, agriculture problems, and microwave, optical and ultrasound imaging and detection of tissues. This paper summarizes several important current problems and applications in geophysical and biological random media that are not often discussed under unified statistical electromagnetic theories. This paper is based on a paper presented at the plenary session of PIERS 2014 Guangzhou conference, August, 2014.

2. HISTORY OF WAVES IN RANDOM MEDIA

Multiple scattering in turbulence and particle have been studied for many years. In astrophysics, and disordered medium, the fundamental theories of the Dyson equation for the first moment, the Bethe-Salpeter equations for the second moment and the Feynman diagram have been developed and have been used as the corner stone of the statistical electromagnetic theory [1,3-5]. Also important are multiple scattering theories of Foldy, Lax, and others [5]. It may be noted that the fundamental studies of statistical electromagnetic theories require extensive theoretical and mathematical work. However, many applications discussed in this paper make use of appropriate approximate theories which may not require the complete mathematical studies and analysis. Thus, the statistical electromagnetic theories encompass most advanced mathematical work and most practical applications.

Radiative transfer theory dating back to Schuster in 1903 and the fundamental transport equation and neutron transport theory have been extensively used in atmospheric and underwater visibility, marine biology, optics in the atmosphere of planets, and stars [1]. It should be noted, however, that the radiative transfer theory is an approximate theory, even though it satisfies the power conservation. Several phenomena such as the Anderson localization, memory effects, and enhanced backscattering require formulation outside the radiative transfer. Recent studies include application to imaging, remote sensing and communication. This requires the integration of wave propagation, scattering, and signal processing, which results in the use of statistical theory in time-reversal and MUSIC (multiple signal classification) imaging techniques.

Multiple scattering by rough surfaces such as oceans are important in imaging, detection and communication near ocean surface. Rough surface scattering studies date back to Rayleigh in 1877 and Rice 1951. Small perturbation, Kirchhoff, small slope, high slope and other approximations have been developed and extensively used. This paper presents a summary of several important recent advances in these problems.

3. MUTUAL COHERENCE FUNCTION: A KEY TO THE STUDY OF WAVES IN RANDOM MEDIA

It is important to understand distinctions between the ordinary deterministic scattering problems where the parameters such as permittivity, size and shape of objects are clearly defined and the random media where the parameters such as dielectric constant and boundaries are known only in statistical terms.

In most ordinary deterministic problems of wave propagation, we deal with the field, amplitude and phase and the intensity in space and time. In deterministic problems, the intensity is the magnitude of the square of the field. However, in random media, the intensity is the sum of the coherent intensity and the incoherent intensity. When studying waves in random media, since the medium is random, it is necessary to characterize the medium as a sum of the average and the fluctuation, or the deviation from the average. The field will need to be expressed as a sum of the average (coherent) and the fluctuating (incoherent or diffuse) fields. Since the fluctuating field is random, we need to express it in terms of the

space-time correlation function. This is called the “Mutual Coherence Function” and is a key to the study of waves in random medium.

Let us consider a field $u(\vec{r}, t)$. The mutual coherence function Γ is the second moment.

$$\Gamma(\vec{r}_1, t_1; \vec{r}_2, t_2) = \langle u(\vec{r}_1, t_1), u^*(\vec{r}_2, t_2) \rangle \quad (1)$$

And the fourth moment is

$$\langle u_1 u_2 u_3^* u_4^* \rangle \quad (2)$$

which also includes the intensity correlation.

$$\langle I_1 I_2 \rangle \quad (3)$$

where $I_1 = |u_1|^2$ and $I_2 = |u_2|^2$ with $u_1 = u_3$ and $u_2 = u_4$.

As an example, consider the wave propagation through a medium with the random dielectric constant e consisting of the average $\langle e \rangle$ and the fluctuation

$$e = \langle e \rangle (1 + \varepsilon_1) \quad (4)$$

where ε_1 is the fluctuating part and

$$[\nabla^2 + k^2(1 + \varepsilon_1)] u = 0, \quad k^2 = k_0^2 \langle \varepsilon \rangle \quad (5)$$

The solution to (5) can be written in the following two series

$$U = U_0 + U_1 + U_2 + \dots = \exp(\psi_0 + \psi_1 + \psi_2 + \dots) \quad (6)$$

The first Born approximation is then given by

$$U_1 = \int G_0(\vec{r}, \vec{r}') V(\vec{r}') U_0(\vec{r}') d\vec{r}' \quad (7)$$

where $V(\vec{r}') = k^2 \varepsilon_1(\vec{r}')$, and G_0 is free space Green's function.

Similarly, we get the first order Rytov solution.

$$\begin{aligned} U &= \exp(\Psi_0 + \Psi_1) \\ \exp(\Psi_0) &= U_0, \quad \Psi_1 = \frac{U_1}{U_0} \\ \Psi_1(\vec{r}) &= \frac{1}{U_0(\vec{r})} \int G_0(\vec{r}, \vec{r}') V(\vec{r}') U_0(\vec{r}') d\vec{r}' \end{aligned} \quad (8)$$

The Rytov solution (8) is commonly used for a line-of-sight propagation for medium with small perturbations. The formulations given in (7) and (8) give the basis for the development of the mutual coherence function given in (9), which is the most important function in dealing with the waves in random media.

The first Rytov solution (8) is approximate and does not conserve the power. The second Rytov solution can be used to conserve the power. A second order modified Rytov solution can be used to express the mutual coherence function.

$$\begin{aligned} \Gamma(\vec{r}_a, \vec{r}_b) &= \Gamma_0 \exp(-D/2) \\ D &= \langle |\psi_a|^2 \rangle + \langle |\psi_b|^2 \rangle - 2 \langle \psi_a \psi_b^* \rangle \end{aligned} \quad (9)$$

where ψ_a and ψ_b are the first order Rytov solution given in (8).

This is consistent with the moment equation solution and the extended Huygens-Fresnel formula. Intensity fluctuation and the scintillation index have been extensively studied [1, 3, 4].

4. IMAGING THROUGH RANDOM MULTIPLE SCATTERING MEDIA

Many imaging problems deal with well-defined objects. Imaging in random media, however, requires studies of the effects of clutter and noise caused by the fluctuations. It is therefore important to clearly understand the statistical theories. Imaging of objects in random media is one of the important practical problems. Examples are imaging and detection of objects in geophysical media and imaging and detection of malignant tissues obscured by surrounding tissues. The effects of clutter on imaging need to be reduced to produce clean images.

One of the promising imaging techniques is the use of time-reversal imaging [8–10]. The wave reflected by the object can trace back and backpropagate through the random medium to form the image. Time-reversal technique has been extensively studied and reported. For a single target, the imaging function ψ is given by [8–10].

$$\Psi = \int d\omega |U|^2 \lambda_1 g_s v_1 \exp(-i\omega t) \quad (10)$$

where $U(\omega)$ is the spectrum of the transmitter, λ_1 the eigenvalue of the eigenvector v_1 , and g_s' the conjugate transpose of the steering matrix g_s .

This is based on Multistatic Matrix \mathbf{K} , Figure 1. Figure 2 shows the time-reversal process to obtain the image. The time-reversal process includes the multistatic matrix \mathbf{K} , and the time-reversal matrix \mathbf{T} and its eigenvalues.

$$\mathbf{T} = \mathbf{K}\mathbf{K}' \quad (11)$$

$$\mathbf{K} = \sum_{m=1}^M \tau_m \mathbf{g}_m \mathbf{g}_m^T \quad \text{where} \quad \mathbf{g}_m = \left[\mathbf{G}(\vec{r}_1, \vec{r}_m, \omega) \quad \mathbf{G}(\vec{r}_2, \vec{r}_m, \omega) \quad \dots \quad \mathbf{G}(\vec{r}_N, \vec{r}_m, \omega) \right] \quad (12)$$

$$(\mathbf{K}\mathbf{v})^* = \sigma \mathbf{v}, \quad \sigma = \text{scattering and diffraction loss} \quad (13)$$

τ_m denotes the scattering strength of the target located at \vec{r}_m .

The eigenvalue equation is given by

$$\begin{aligned} \mathbf{K}^* \mathbf{K} \mathbf{v} &= \lambda \mathbf{v} \\ \lambda &= \frac{\|\mathbf{K}\mathbf{v}\|^2}{\|\mathbf{v}\|^2} = \text{real and positive} = \frac{\text{received power}}{\text{input power}} \end{aligned} \quad (14)$$

Time Reversal Imaging is related to DORT (Decomposition of Time Reversal Operator) and SVD (Singular Value Decomposition) [8].

It is important to note that the study of imaging in random medium requires extensive interplay between the propagation and the signal processing. Several imaging techniques are summarized here [9].

$$\text{TR imaging} = \int d\omega_1 d\omega_2 U_1^2 U_2^2 \lambda_1^2 \sum_i \sum_j \langle G_i G_j^* \rangle \langle G_{si}^* G_{sj} \rangle \quad (15)$$

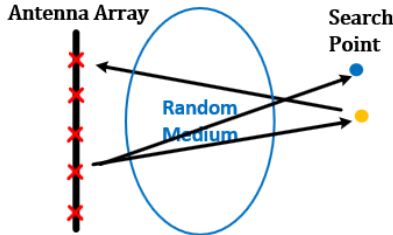


Figure 1. How to image through random multiple scattering media.

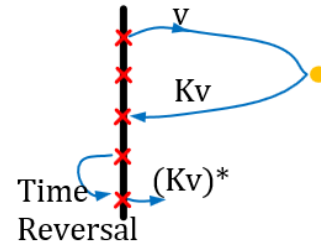


Figure 2. Time reversal process.

$$\text{TR MUSIC} = \frac{1}{\sum_{p=M+1}^{N-1} \int d\omega U^2 |[g_s]'v_p|} \tag{16}$$

$$\text{Capon} = \frac{1}{\int d\omega |U|^2 [g_s(\omega_1)]' [R]^{-1} [g_s(\omega_2)]'} \tag{17}$$

$$\text{Modified Beamform} = \iint d\omega_1 d\omega_2 U_1 U_2 \sum_i \sum_j \sum_p \sum_q \langle G_i G_j G'_p G'_q \rangle \langle G_{si} G_{sj} G'_{sp} G'_{sq} \rangle \tag{18}$$

$$\text{SAR} = \iint d\omega_1 d\omega_2 |U_1|^2 |U_2|^2 \langle G_i^2(\omega_1) G_j^{*2}(\omega_2) \rangle \langle G_{si}^{*2}(\omega_1) G_{sj}^2(\omega_2) \rangle \tag{19}$$

G is Green’s function. N denotes the number of array elements and M is the number of the targets. G in (15) is the stochastic Green’s function, and g_s is the steering vector. R in (17) is the correlation matrix noted in [9], which is used in minimum variance beamforming [22].

A key is the stochastic Greens’ function and the mutual coherence function in random medium such as $\langle G_i G_j^* \rangle$ [9].

Numerical comparisons are given in Figure 3 [9].

Parameters in Figure 3 shows that OD (optical depth) = 1.0, $\Delta\omega$ (bandwidth) = 0.01 of carrier frequency, N = number of array elements, $L = 50\lambda$ distance between the array and the target.

Figure 3 shows comparison of images using different imaging techniques. Transmitter and receiver arrays are at the left side where the distance is zeros. The details are shown in [9] which covers different OD (optical depth).

Super resolution is an interesting phenomenon in the time-reversed imaging. The wave propagates through random medium and is reflected by the object. As the wave propagates through the multiple scattering medium, the coherent distance ρ_0 at the target is reduced and becomes less than the spot size W_0 . Then the imaging size of the object W is dominated by the coherent size rather than the spot size. This can also be viewed as apparent increase of the transmitter aperture size W_t . This is sketched in Figure 4.

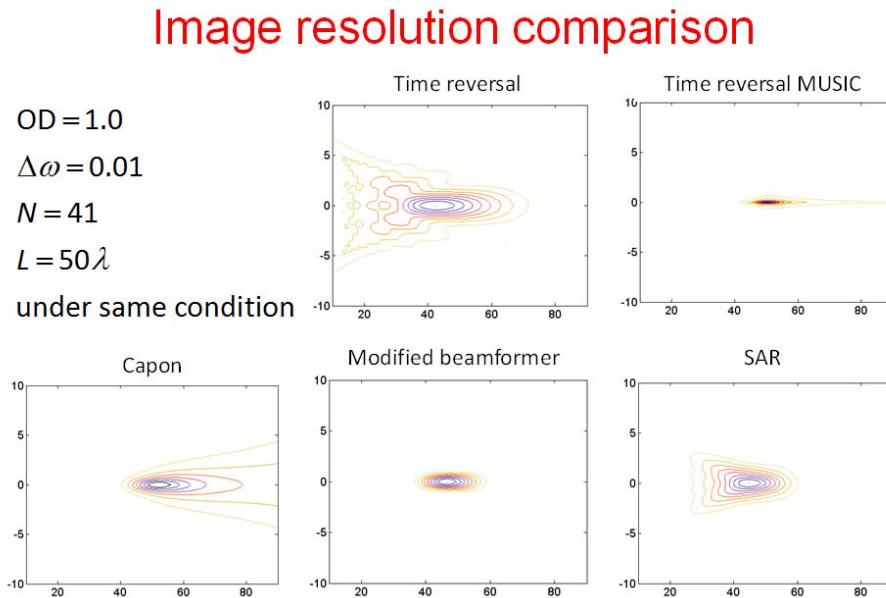


Figure 3. Image resolution comparison.

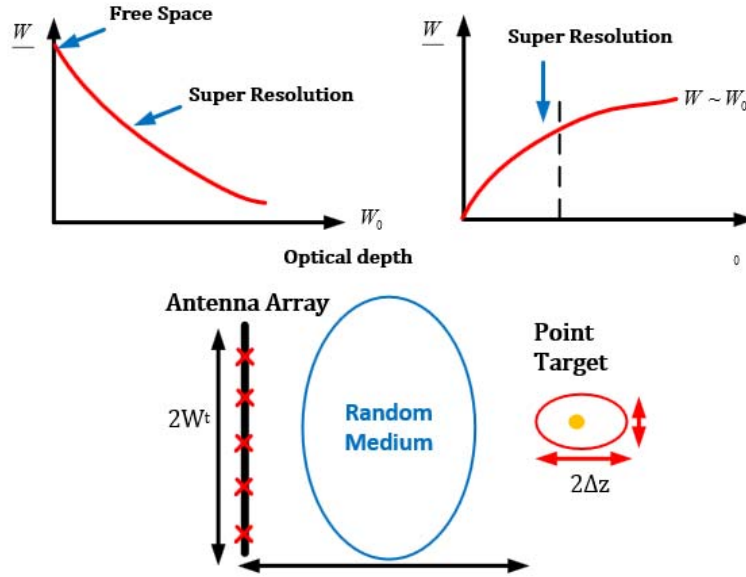


Figure 4. Super resolution.

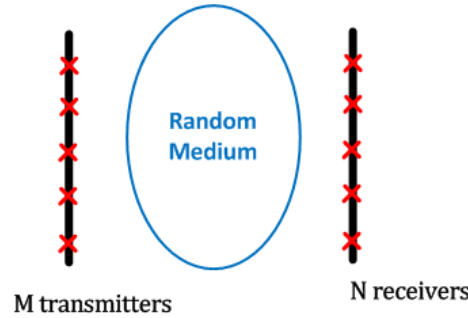


Figure 5. How to include random media effects on MIMO (Multiple input-multiple output) communication channel capacity?

5. COMMUNICATION THROUGH RANDOM MEDIA

Communications through various media and obstacles are important in many practical problems such as the communications in the atmosphere, underwater, and terrains with various obstacles, which often severely affect communications. In many communication problems, main emphasis is usually placed on the input and output and their statistical characterizations.

In some cases, the channel characterizations are expressed by using a certain statistical assumptions such as circular complex Gaussian and other random variables [11]. It is therefore desirable to include actual physical media characteristics in the communication problems. These physical characterizations include the atmospheric turbulence characteristics and rain rate, particle size distributions and others.

The propagation problems normally include the medium characterization and therefore it is desirable to formulate the communication problems by integrating propagation and signal processing which include the physical characterization of the medium. In order to express the physical characterizations of the medium, it is necessary to express the medium effects on propagation by formulating the stochastic Green's function.

As an example, consider the MIMO communication channel [11, 12], Figure 5. Channel capacity is

- 60 GHz, L=500m, Bandwidth = 500 kHz, thermal noise

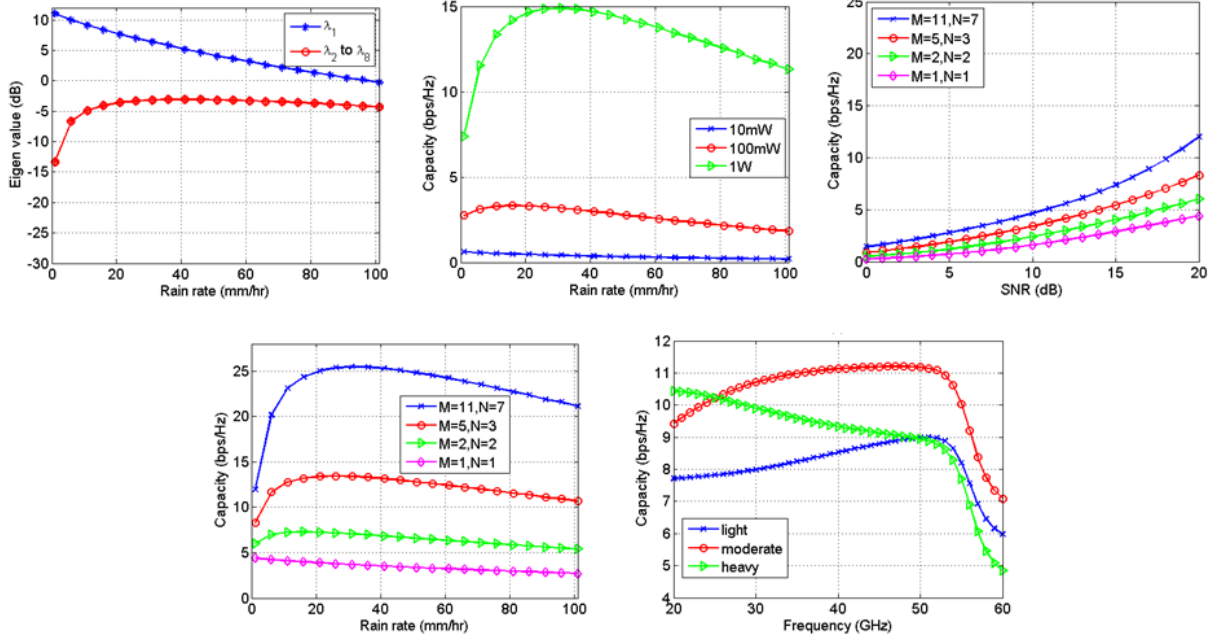


Figure 6. Examples: channel capacity through rain.

approximately given by

$$\begin{aligned}
 C &\approx \log_2 \left[\det \left(\mathbf{I} + \left(\frac{\rho}{M} \mathbf{H} \mathbf{H}^H \right) \right) \right] \text{ bps/Hz} \\
 \rho &= P/N = \text{Signal to Noise Ratio} \\
 \mathbf{H} &= \text{Normalized Channel Matrix}
 \end{aligned}
 \tag{20}$$

\mathbf{I} is the unit matrix, and \mathbf{H}^H is the conjugate transpose of the matrix \mathbf{H} .

We can then obtain an upper bound of the mean capacity.

$$\begin{aligned}
 C &\leq C_{up} = \log_2 \left[\det \left(\mathbf{I} + \left(\frac{\rho_t}{M\sigma^2} \langle \mathbf{T} \mathbf{T}' \rangle \right) \right) \right], \quad T_{mn} = \text{channel transfer matrix} = F_{rn} F_{tm} g_{mn} (\vec{r}_n, \vec{r}_m) \\
 &= \sum_i \log_2 \left[\det \left(\mathbf{I} + \left(\frac{\rho_t}{M\sigma^2} \lambda_i \right) \right) \right], \quad \lambda_i = \text{eigenvalues of } \langle \mathbf{T} \mathbf{T}' \rangle
 \end{aligned}
 \tag{21}$$

$$\langle \mathbf{T} \mathbf{T}' \rangle_{mn'} = F^2 \sum_i \Gamma_{mn'}, \quad \Gamma_{mn'} = \text{Mutual Coherence function} = \langle g_{nm} g_{mn'}^* \rangle$$

F_r and F_t are the antenna characteristics of the receiver and transmitter respectively and is given by λ (gain) [12].

This includes the channel transfer matrix consisting of the antenna characterization, the gain, and the eigenvalues of $\langle \mathbf{T} \mathbf{T}' \rangle$. Figure 6 shows an example of the channel capacity of 60 GHz communication through rain. It shows the increase of the channel capacity due to the number of antenna elements, the rain rate and the frequency [12].

6. BIO-ELECTROMAGNETICS AND HEAT DIFFUSION IN TISSUE

Biological tissues are inherently random. Medium characteristics such as permittivity are inhomogeneous and vary in time and space and require applications of statistical electromagnetic

theories. In bio-electromagnetics, we are dealing with several issues including (1) Static-microwave-TeraHertz (0.1 to 10 THz), (2) medical, diagnosis, cell phones, hyperthermia, exposure, imaging, thermotherapy, (3) SAR (Specific Absorption Rate), thermotherapy, bio-effects of magnetic field, eddy current, and (4) heat diffusion.

Here, we briefly outline the heat diffusion in tissue due to microwave radiation [13]. Consider the incident power flux (mW/cm^2) in tissue given by SAR (specific absorption rate, watts/kg). The heat flow \bar{F} is governed by

$$\begin{aligned} \rho C_s \frac{\partial T}{\partial t} + \nabla \bar{F} &= q, \quad \bar{F} = -k \nabla T, \quad K = \text{thermal conductivity} \\ \rho &= \text{density}, \quad C_s = \text{specific heat}, \quad q = L - C, \quad C = \text{cooling function} \\ L = \text{EM power loss} &= \frac{\sigma |E|^2}{2}, \quad \text{SAR} = \frac{L}{\rho} \text{ (watts/kg)} \end{aligned} \quad (22)$$

The temperature distribution obeys the diffusion equation.

$$\frac{\partial T}{\partial t} = a^2 \nabla^2 T + \frac{q}{\rho C_c}, \quad a = \sqrt{\frac{K}{\rho C_s}} = \text{diffusion coefficient} \quad (23)$$

An example of the boundary condition is Newton Cooling Law

$$\begin{aligned} -K \frac{\partial T}{\partial n} &= E(T - T_e), \quad T_e = \text{environmental temperature} \\ E/K &= \text{Biot's number} \end{aligned} \quad (24)$$

Several other boundary conditions have also been proposed.

These Equations (22)–(24) form the basis of the heat diffusion in tissues. As noted in [13], there have been extensive works reported on the microwave heating of tissues, which are important in thermotherapy and heat generated by microwave exposure.

7. OPTICAL AND ULTRASOUND IN TISSUES

As noted in the last section, biological tissues are inherently random, requiring applications of statistical theories. Both optical and ultrasound waves are used to image and probe the tissue characterizations. There are significant differences between optical and ultrasound imaging. In optics, scattering is much greater than absorption and therefore diffusion dominates. In ultrasound, scattering is much smaller than absorption and therefore first order scattering dominates. This can be summarized as follows. Figure 7 shows the scattering process in scattering.

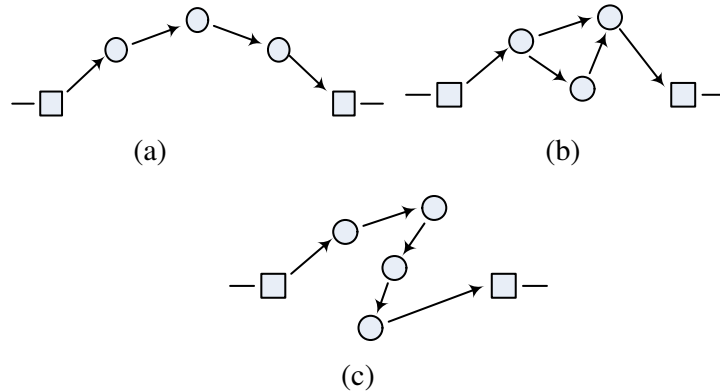


Figure 7. Scattering process: (a) first order scattering (ultrasound in tissue), (b) multiple scattering (microwave, millimeterwave, optical, in fog, rain, radiative transfer, turbulence, rough surfaces, ionospheric turbulence, ocean acoustics), (c) diffusion (random walk, tissue optics, photon density waves).

8. OPTICAL DIFFUSION IN TISSUES AND PHOTON-DENSITY WAVES

As stated in last section, in optics, scattering dominates in tissues and therefore diffusion dominates. The diffusion equation can be derived from radiative transfer equations as shown here [1].

$$\begin{aligned}
 (\nabla^2 + k_d^2) U_d &= \text{source term} \\
 k_d^2 &= -3\mu_a\mu_{tr} \\
 \mu_a &= \text{absorption coefficient} \\
 \mu_{tr} &= \text{transport scattering coefficient} \\
 &= \mu_t - g\mu_s, \quad g = \text{anisotropy facto}
 \end{aligned}
 \tag{25}$$

Boundary condition

$$U_d - \frac{2}{3\mu_{tr}} \frac{\partial}{\partial n} U_d = 0
 \tag{26}$$

The boundary condition is approximate because the diffusion equation itself is approximate. The resolution of images in diffusion medium is poor. However, it is possible to make use of the modulated intensity wave, called the “photon density” wave, which gives the resolution in the order of the wavelength of the modulated intensity wave.

$$\begin{aligned}
 I &= I_c + I_m e^{-i\omega_m t} \quad \text{Modulated Intensity} \\
 (\nabla^2 + k_d^2) U &= 0 \\
 k_d^2 &= -3 \frac{\mu_a}{\mu_{tr}} + i \frac{\omega_m}{C_b^2} 3\mu_{tr} \\
 C_b &= \text{light velocity in background medium}
 \end{aligned}
 \tag{27}$$

It can be shown that, for small absorption, the wavelength of the modulated intensity is of the order of centimeter.

9. ULTRASOUND SCATTERING IN BLOOD AND TISSUES

Frequencies used ultrasound in biomedical problems range approximately from 1 MHz to 50 MHz (wavelength: 3 cm to 0.6 mm). The sizes of red blood cells are approximately 3 μm and therefore the cell sizes are much smaller than a wavelength and Rayleigh scattering applies. The scattering amplitude of a red blood cell and the differential cross section per unit volume of blood are given by [1, 14].

Scattering Amplitude

$$f(\hat{o}, \hat{i}) = \frac{k^2 a^3}{3} \left(\frac{k_e - k}{k} + \frac{3\rho_e - 3\rho}{2\rho_e + 3\rho} \cos\theta \right)
 \tag{28}$$

k is the wave number in the medium with density ρ .

k_e and ρ_e are the wavenumber and density of the blood cell.

a is the equivalent radius of the single red blood cell. Figure 9.

Differential scattering cross section per unit volume:

$$\begin{aligned}
 \sigma(\hat{o}, \hat{i}) &= \frac{H f_p(H)}{V_e} \left| f(\hat{o}, \hat{i}) \right|^2 \\
 H &= \text{hemotocrit} \\
 f_p(H) &= \text{packing factor} \\
 &\approx \frac{(1 - H)^4}{(1 + 2H)^2} \quad (\text{hard sphere-Percus-Yevick}) \\
 V_e &= \text{volume of single cell}
 \end{aligned}
 \tag{29}$$

The percent volume occupied by blood cells (fractional volume) is called “hematocrit”. Human hematocrit is approximately 40% ($H = 0.4$). The differential cross section per unit volume is

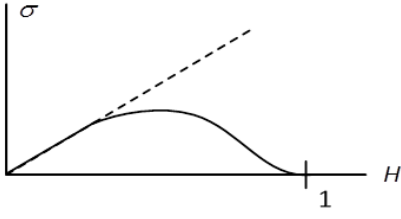


Figure 8. Differential scattering cross section per unit volume.

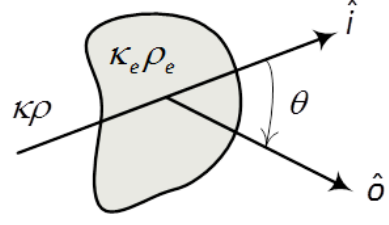


Figure 9. Ultrasonic in tissues.

proportional to H , but when H exceeds 10%~20%, the scattering cross section decreases as shown in Figure 8 due to the packing factor. The packing factor has been studied extensively in “dense media” theory [15].

The differential cross section per unit volume of tissues are evaluated by the compressibility fluctuation and the density fluctuation. This is sketched below [1, 14].

$$f(\hat{o}, \hat{i}) = \frac{k^2}{4\pi} \int_{\delta V} (\gamma_\kappa + \gamma_\rho \cos \theta) \exp(i\bar{k}_s \cdot \bar{r}') dV'$$

$$\gamma_\kappa = \frac{\kappa_e - \kappa}{\kappa} = \text{compressibility fluctuation}, \quad (30)$$

$$\gamma_\rho = \frac{\rho_e - \rho}{\rho} = \text{density fluctuation},$$

$$\bar{k}_s = k(\hat{i} - \hat{o}), \quad \kappa_s = 2k \sin(\theta/2)$$

$$\sigma_d(\hat{o}, \hat{i}) = \frac{\langle f f^* \rangle}{\delta V} = \frac{\pi}{2} k^4 [S_\kappa(k_s) + S_\rho(k_s) \cos^2 \theta + 2S_{\kappa\rho}(k_s) \cos \theta] \quad (31)$$

$$S_\kappa(k_s) = \frac{1}{(2\pi)^3} \int \langle \gamma_\kappa(\bar{r}_1) \gamma_\kappa(\bar{r}_2) \rangle \exp(i\bar{k}_s \cdot \bar{r}_d) dV_d = \text{Spectral density}$$

10. RADIATIVE TRANSFER AND ITS LIMITATIONS

The radiative transfer theory was proposed by Schuster in 1905 to explain the radiation through a foggy atmosphere [1]. This was refined further by Chandrasekharin in 1950 and others in application to astrophysical problems. It is closely related to neutron transport theory and is equivalent to Boltzman’s equation used in kinetic theory of gases.

Radiative transfer theory has been extensively used for microwave remote sensing of geophysical media [15, 16]. The narrowband radiative transfer with time dependence is given by

$$\frac{dI}{dz} = -\gamma_t I - \frac{\partial}{\partial t} I + \int SI' d\Omega' \quad (32)$$

If broadband and dispersion are included, we have two frequency radiative transfer equations

$$I = I(\omega_1, \omega_2) \quad (33)$$

$$\frac{dI}{dz} = i[K(\omega_1) - K^*(\omega_2)]I + \int SI' d\Omega' \quad (34)$$

$$\frac{dI}{dz} \approx \left[i \frac{\omega_d}{v_g} - \gamma_t \right] I + \int SI' d\Omega' \quad (35)$$

Equations (32)–(35) are the conventional radiative transfer equation. I is the specific intensity, and S is the scattering phase function. The radiative transfer theory has been developed over the years and represents the propagation and scattering of the intensities in random media.

If we include the polarization effects, we have two-frequency vector radiative transfer with the two-frequency Stokes vector. It must be kept in mind that the radiative transfer is an approximate theory even though it satisfies the necessary condition of the conservation of power. However, it should be noted that the radiative transfer does not satisfy the reciprocity in some cases [17].

11. COHERENCE IN MULTIPLE SCATTERING — DOUBLE PASSAGE EFFECTS

As a wave propagates through multiple scattering medium, the original incident coherent wave suffers from scattering and the coherent wave diminishes while the incoherent wave increases, as shown in Figure 7. This means that the coherence in the original incident wave disappears. This is a view that we normally expect. However as indicated in the last section, there are some conditions, under which the coherence can be maintained even under multiple scattering [17, 18]. The coherence in multiple scattering is unexpected from conventional point of view. This is new phenomena which have recently been discussed, and this caused intense theoretical study and practical applications.

We consider examples of this phenomenon of coherence in multiple scattering. First is the double passage effect. As shown in Figure 10, as we observe a target through turbulence, we may expect the decrease of the target cross section. It was, however, shown and experimentally verified that the apparent target cross section can increase as much as 2 or 3 times the free space cross section.

The radar equation considering turbulence is given by

$$\begin{aligned}
 P_r &= P_t \frac{\lambda G^2}{(4\pi)^3 R^4} \sigma_{ap}, \\
 \text{Normalized } \langle e_u \rangle &= \langle e_d \rangle = 1 \\
 \sigma_{ap} &= \text{apparent target cross section} = \sigma_b \langle |e_u e_d|^2 \rangle
 \end{aligned}
 \tag{36}$$

Equation (36) is the conventional random equation, except that the target cross section is modified by turbulence and becomes the apparent cross section.

Here we show this by noting radar equations including the target cross section which is proportional to the square of upward and downward waves. We also show that the apparent cross section is twice the free space cross section if the intensity is Rayleigh distributed.

$$\begin{aligned}
 \sigma_{ap} &= \sigma_{ap} \langle |e|^4 \rangle, \quad e_u = e_d \quad \text{reciprocity} \\
 \langle |e|^4 \rangle &= \langle I^2 \rangle, \\
 \langle I^N \rangle &= N! \langle I \rangle^N = 2 \langle |e|^2 \rangle = 2 \quad \text{for Rayleigh distribution} \\
 \sigma_{ap} &= 2\sigma_b
 \end{aligned}
 \tag{37}$$

The scintillation index (variance of the intensity fluctuation) is given by

$$S_4^2 = \frac{\langle (I^2 - \langle I^2 \rangle)^2 \rangle}{\langle I^2 \rangle^2} = \frac{4! - 2^2}{2^2} = 5 \quad (\text{Rayleigh})
 \tag{38}$$

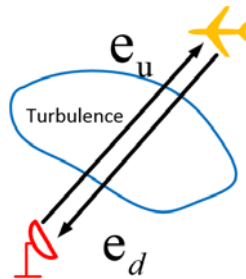


Figure 10. Double passage effects.

Experimental evidence for S_4^2 and σ_{ap} show that

$$\begin{aligned} \sigma_{ap} &= (3 \text{ to } 2 \text{ to } 1) \\ S_4^2 &= \left(\frac{32}{3} \text{ to } 5 \text{ to } 0 \right) = (10.7 \text{ to } 5 \text{ to } 0) \end{aligned} \tag{39}$$

This also includes the effects of other distributions such as Nakagami distribution on the scintillation index [18].

12. BACKSCATTERING ENHANCEMENT AND ANDERSON LOCALIZATION

In 1984, optical experiment (Kuga-Ishimaru) and theory (Tsang-Ishimaru) were reported and shown to be “Anderson localization” of electron-localization in disordered material (absence of diffusion of electrons) [17, 18].

As shown in Figure 11, multiple scattered wave from particles and its counter-propagating wave are interfered constructively in the exact backscattering direction, producing twice the intensity obtained from the radiative transfer [18]. This is called the “backscattering enhancement” and it also happens for scattering by rough surfaces as shown in Figure 12 and Figure 13.

13. MEMORY EFFECTS

In 1988, Feng proposed that even under multiple scattering, the scattered waves remember the directions of incident waves showing angular and frequency correlations of the scattered waves along the MEMORY

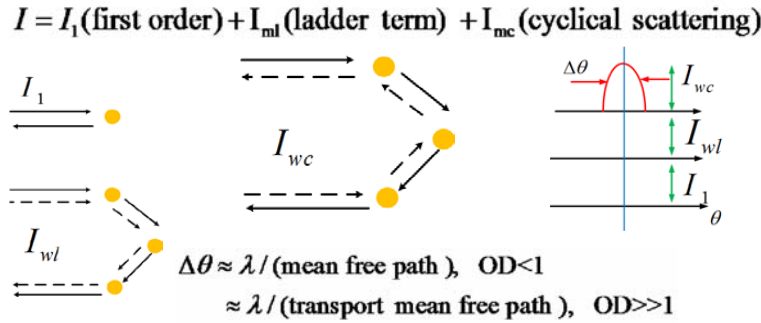


Figure 11. Enhanced backscattering occurs for particle scattering, rough surface scattering, and is “weak Anderson localization”.

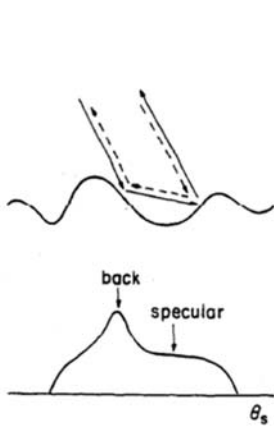


Figure 12. Backscattering enhancement from rough surfaces.

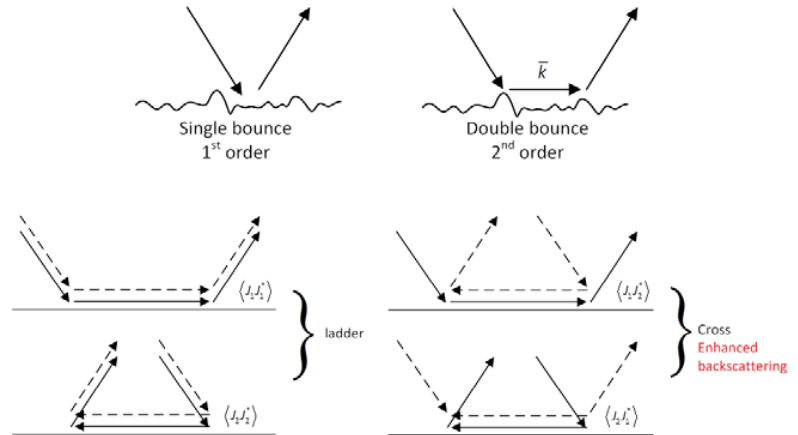


Figure 13. Backscattering enhancement from rough surfaces.

LINES in the memory diagram.

This is called the memory effects and extensive theoretical and experimental work has been reported. Figure 14 shows this effect for rough surface scattering. Figure 15 shows analytical and experimental study on the memory diagram under different incident and scattering angles with different frequencies. It is possible to reduce the rough surface scattering clutter. This has been reported at IEEE APS-USRI meeting in July 2014.

- Two incident waves with two frequencies $\omega \neq \omega'$ and two different incident angles.
- Correlations of two different scattered waves with two different frequencies at two scattering angles

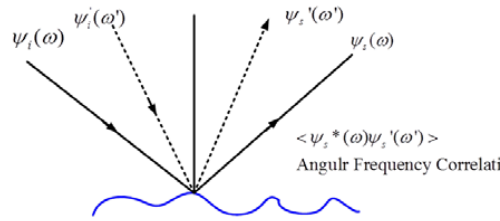


Figure 14. Memory effects.

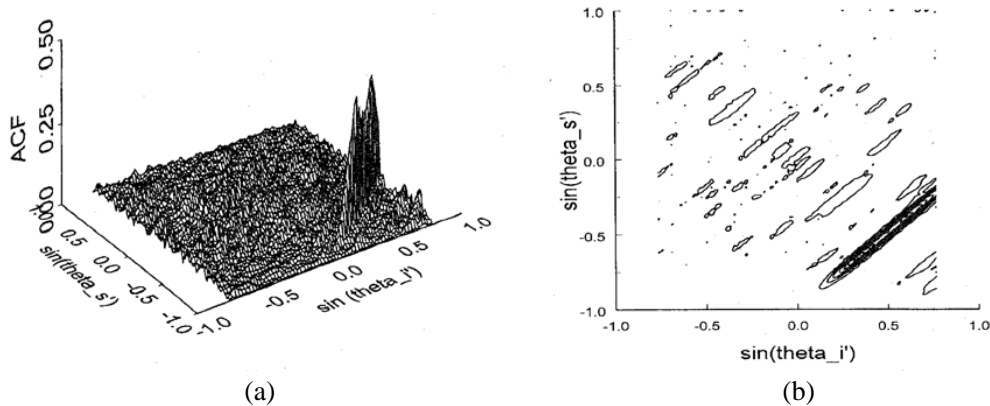


Figure 15. (a) Memory diagram and (b) memory line.

Relations with transformation EM (Cloaking)

Free Space

$$\begin{aligned} \nabla \times \vec{E} &= j\omega\mu_0 \vec{H} \\ \nabla \times \vec{H} &= -j\omega\epsilon_0 \vec{E} \\ \nabla \times \nabla \times \vec{E} &= \omega^2 \mu_0 \epsilon_0 \vec{E} \end{aligned}$$

$\frac{\epsilon}{\epsilon_0} = \frac{\mu}{\mu_0} = \frac{AA^T}{\det A}$

A = Transformation matrix

- Impedance is not changed
- Anisotropic impedance matched media
- Rough surface with free space \rightarrow flat surface with random media

Rough Surface:

Free Space (x, y, z)

Flattened Surface:

Inhomogeneous & Anisotropic Media

$z' = z - \zeta(x, y)$
 $x' = x \quad y' = y$

• **A = Transformation Matrix**

$$A = \begin{bmatrix} \frac{\partial x'}{\partial x} & \frac{\partial x'}{\partial y} & \frac{\partial x'}{\partial z} \\ \frac{\partial y'}{\partial x} & \frac{\partial y'}{\partial y} & \frac{\partial y'}{\partial z} \\ \frac{\partial z'}{\partial x} & \frac{\partial z'}{\partial y} & \frac{\partial z'}{\partial z} \end{bmatrix} = \begin{bmatrix} 1 & 0 & 0 \\ 0 & 1 & 0 \\ -\frac{\partial \zeta}{\partial x} & -\frac{\partial \zeta}{\partial y} & 1 \end{bmatrix}$$

• $\frac{\epsilon}{\epsilon_0} = \frac{\mu}{\mu_0} = \frac{AA^T}{\det A} = \begin{bmatrix} 1 & 0 & -\frac{\partial \zeta}{\partial x} \\ 0 & 1 & -\frac{\partial \zeta}{\partial y} \\ -\frac{\partial \zeta}{\partial x} & -\frac{\partial \zeta}{\partial y} & \left(\frac{\partial \zeta}{\partial x}\right)^2 + \left(\frac{\partial \zeta}{\partial y}\right)^2 + 1 \end{bmatrix}$

Figure 16. Relations with transformation EM (cloaking).

14. APPLICATION OF TRANSFORMATION EM FOR ROUGH SURFACE IMAGING PROBLEM

Extensive works have been reported on Transformation Electromagnetics for cloaking possibilities [19, 20]. Here we discuss different use of Transformation EM to transform free space above rough surface to random medium above flat surface [19]. This is shown in Figure 16. This technique has been used to image a target located close to the rough surface when the transmitter is located close to the rough surface.

15. SEISMIC CODA

Statistical electromagnetic theory can be used to apply to the study of seismic coda, which may be used to probe earth inhomogeneities and information about seismic source and media [21]. Seismic waves include P (pressure wave, longitudinal wave) with a velocity of 5~6 km/s, S (shear wave, transverse wave) with a velocity of 3 km/s, and if the source is close to the surface, Rayleigh surface waves may be excited with a velocity of close to 90% of an S wave.

The lithosphere is the region of the earth down to about 100 km, which consists of the crust and the uppermost mantle and the crust is generally heterogeneous on scales of a few km to tens of km. The local earthquakes propagate through the lithosphere over distances of 100 km with frequencies from 1~30 Hz. The initial appearance of the wave is followed by the wave train, called “Coda”, which is the incoherent wave scattered by the heterogeneous earth. The Coda is important to probe information on the earthquake source and media.

The characterizations of the coda have been studied using several techniques including simple scattering, parabolic equation method, and radiative transfer depending on the distance and the time duration. The total scattering coefficients for S -coda is in the range of 10^{-2} km^{-1} for frequencies of 1~30 Hz. This is equivalent to the mean free path of 100 km and the time duration of $(100/4) = 25 \text{ s}$ for S -wave velocity of 4 km/s. More complete discussion can be found in Sato and Fehler [21].

16. CONCLUSION

This paper gives a review of the application of the statistical electromagnetic theories to several research areas on imaging through clutter, geophysical remote sensing, time-reversal imaging, and communication through clutter. Next we discuss biological applications in electromagnetics diffusion in tissues. Radiative Transfer and its limitation and coherence in multiple scattering, Anderson localization, memory effects, and double passage effects are discussed. The paper includes an application of Transformation Electromagnetics, and seismic coda. These are only a small part of many potential applications of statistical electromagnetic theory. This field is one of the most challenging theoretical and mathematical problems including a vast field of practical applications in geophysical, biological and environmental problems.

ACKNOWLEDGMENT

This work was supported by NSF (ECCS0925034) and ONR (N00014-07-1-0428).

REFERENCES

1. Ishimaru, A., *Wave Propagation and Scattering in Random Media*, IEEE Press-Oxford University Press Classic Reissue, IEEE Press, Piscataway, NJ, and Oxford University Press, Oxford, England, 1997.
2. Ishimaru, A., *Electromagnetic Wave Propagation, Radiation, and Scattering*, 637, Prentice Hall, Englewood Cliffs, NJ, 1991.
3. Tatarskii, V. I., “The effects of the turbulent atmosphere on wave propagation,” TT-68-50464, US Department of Commerce, Springfield, Virginia, 1971.

4. Tatarskii, V. I., A. Ishimaru, and V. U. Zavorotny, *Wave Propagation in Random Media (Scintillation)*, SPIE Press and Bristol, Institute of Physics Publishing, Bellingham, WA, England, 1993.
5. Tsang, L. and J. A. Kong, *Scattering of Electromagnetic Waves, Advanced Topics*, Vol. 26, John Wiley & Sons, 2004.
6. Ulaby, F. T., R. K. Moore, and A. K. Fung, *Microwave Remote Sensing: Microwave Remote Sensing Fundamentals and Radiometry*, Vol. I, Advanced Book Program/World Science Division, Addison-Wesley Publishing Company, 1981.
7. Lin, J. C., Ed., *Electromagnetic Fields in Biological Systems*, CRC Press, 2011.
8. Devaney, J., *Mathematical Foundations of Imaging, Tomography and Wavefield Inversion*, Cambridge University Press, 2012.
9. Ishimaru, S. J. and Y. Kuga, "Imaging through random multiple scattering media using integration of propagation and array signal processing," *Waves in Random Media*, Vol. 22, No. 1, 29–39, Feb. 2012.
10. Prada, C. and M. Fink, "Eigenmodes of the time reversal operator: A solution to selective focusing in multiple-target media," *Wave Motion*, Vol. 20, No. 2, 151–163, 1994.
11. Paulraj, A., R. Nabar, and D. Gore, *Introduction to Space-time Wireless Communications*, Cambridge University Press, 2003.
12. Ishimaru, A., et al., "A MIMO propagation channel model in a random medium," *IEEE Transactions on Antennas and Propagation*, Vol. 58, No. 1, 178–186, 2010.
13. Khaled, A.-R. A. and K. Vafai, "The role of porous media in modeling flow and heat transfer in biological tissues," *International Journal of Heat and Mass Transfer*, Vol. 46, No. 26, 4989–5003, 2003.
14. Shung, K. K. and G. A. Thieme, *Ultrasonic Scattering in Biological Tissues*, CRC Press, Boca Raton, 1992.
15. Tsang, L., J. A. Kong, and R. T. Shin, *Theory of Microwave Remote Sensing*, John Wiley and Sons, 1985.
16. Ulaby, F. T., R. K. Moore, and A. K. Fung, *Microwave Remote Sensing Active and Passive*, Vol. III, Advanced Book Program/World Science Division, Addison-Wesley Publishing Company, 1981.
17. Legendijk, A. and B. A. Van Tiggelen, "Resonant multiple scattering of light," *Physics Reports*, Vol. 270, No. 3, 143–215, 1996.
18. Ishimaru, A., "Backscattering enhancement — From radar cross sections to electron and light localizations to rough surface scattering," *IEEE Antennas Propagation Magazine*, Vol. 33, 7–11, 1991.
19. Ishimaru, A., C. Zhang, M. Stoneback, and Y. Kuga, "Time-reversal imaging of objects near rough surfaces based on surface flattening transform," *Waves in Random and Complex Media*, Vol. 23, No. 3, 306–317, 2013.
20. Leonhardt, U. and T. Philbin, *Geometry and Light: The Science of Invisibility*, Courier Dover Publications, 2012.
21. Sato, H. and M. C. Fehler, *Seismic Wave Propagation and Scattering in the Heterogeneous Earth*, Springer, New York, 1998.
22. Johnson, D. H. and D. E. Dudgeon, *Array Signal Processing: Concepts and Techniques*, Prentice Hall, Englewood Cliffs, NJ, 1993.